Int. J. Heat Mass Transfer Vol. 31, No. 5, pp. 1035–1048, 1988
Printed in Great Britain

0017–9310/88 $3.00 + 0.00
Pergamon Press plc

Radiative influence on the stability of fluids enclosed in vertical cavities

G. DESRAYAUD
Laboratoire de Thermique, C.N.A.M., 292 rue Saint-Martin, 75141 Paris Cedex 03, France

and

G. LAURIAT
Universite de Nantes, 2 rue de la Houssinière, 44072 Nantes Cedex, France

(*Received* 16 *June* 1987)

Abstract—This paper examines the stability of natural convection of a radiating fluid contained in a vertical slot having isothermal side walls at different temperatures. An absorbing–emitting, non-grey but non-scattering fluid is considered and the P1 approximation is used to describe the radiative flux in the energy equation. The base flow equations and the linear stability equations were solved by a spectral tau method. The effect of radiation on the critical values are presented as functions of the interaction parameter, the optical thickness of the fluid, the non-greyness parameter and the wall emissivities over a wide range of stratification parameter. The energetics of the critical disturbance modes were also calculated. For all the cases investigated, it is found that the instabilities set in as a single travelling wave the moving direction of which depends on the wall emissivities. The predictions of the stability analysis are verified by finite difference calculations of multicellular flows of radiating fluids.

INTRODUCTION

THIS PAPER reports on a study of thermal convective flows of radiating gases enclosed in vertical slots with side walls maintained at uniform but different temperatures. For high aspect ratio cavities, the flow may become unstable in the conduction regime and it undergoes a transition to a multicellular flow pattern. This behaviour has been studied theoretically by using the linear stability analysis and the minimum Grashof number, for which a one-dimensional base flow becomes unstable, has been determined accurately for a large range of Prandtl numbers [1–4]. At moderate Prandtl numbers ($Pr < 12.7$), only the stationary instabilities exist for the conduction regime in a fluid layer contained between two isothermal plates [4, 5]. The instability is hydrodynamic in its origin and the critical Grashof number is nearly independent of Prandtl number. However, when asymmetries occur in the base flow [6], the instability sets in as a single wave travelling along one of the plates.

To study the stability in the transition as well as boundary layer regimes, the effects of the vertical temperature gradient must be taken into account. This can be done by introducing into the analysis an additional parameter, namely the stratification parameter $m = (\gamma Ra/4)^{0.25}$ where γ is an arbitrary constant which gives the state of temperature stratification of the core in dimensionless form [5, 7]. It has been shown by Bergholz that the magnitude of m and the value of Pr have a strong influence upon the type and character of the instability. For Prandtl numbers close to unity, a change in the mode of instability occurs if m exceeds a value of the order of $m_1 \simeq 5$: the critical disturbance modes are stationary if $m < m_1$ and travelling waves if $m > m_1$. These results can be applied not only for a vertical layer but also for cavities the aspect ratios of which are moderately large provided that a uniform stable vertical temperature gradient is present in the core. For example, travelling waves were observed experimentally by Schinkel [8] for air-filled cavities with aspect ratios ranging from 5 to 9. Agreements between theoretical and numerical results have also been noted in the works of Jones [9], Lee and Korpela [10], Lauriat and Desrayaud [11] among others.

While the Benard problem of radiating fluids has received considerable attention in the past, the vertical case has been much less studied. The interaction of radiation and convection in the boundary layer regime has been analytically and experimentally examined by Bratis and Novotny [12]. The experimental data are compared to a boundary layer type analysis and special attention is turned to the heat transfer calculations and to the accuracy of radiation-gas models rather than on the influence of the interaction upon the flow regimes. More recently, Kurosaki *et al.* [13] numerically and experimentally studied combined radiation and natural convection using carbon dioxide as a radiating medium in a cavity of moderate aspect ratio. The effects of radiation on the various flow regimes were investigated numerically by Lauriat [14, 15] both for grey fluids and for non-grey gases.

NOMENCLATURE

a	thermal diffusivity
A	aspect ratio of the cavity, H/D
D	width
Gr	Grashof number, $g\beta\Delta T' D^3/\nu^2$
H	height of the cavity
I_0	first moment of the radiation intensity
k_m	mean extinction coefficient
n	index of refraction
p	pressure
P_0	interaction parameter, $k_m\lambda/n^2\bar{\sigma}T_m'^3$
Pr	Prandtl number, ν/a
$\mathbf{q}_r$	radiative heat flux vector of components (q_{rx}, q_{rz})
Ra	Rayleigh number, $Gr\,Pr = g\beta\Delta T' D^3/a\nu$
T	dimensionless temperature
T_m	dimensionless mean temperature
$T_n^*(x)$	shifted Chebyshev polynomial of the first kind (nth order)
$\Delta T'$	temperature difference between the side walls
$\mathbf{V}$	velocity vector of components (v, w)
x	dimensionless horizontal coordinate, x'/D
z	dimensionless vertical coordinate, z'/D.

Greek symbols

α	dimensionless wave number in the z-direction
β	coefficient of thermal expansion
γ	vertical dimensionless temperature gradient, $\partial T/\partial z$
ε_i	emissivity of wall i; $i = 1, 2$
η	non-greyness factor
λ	thermal conductivity
ν	kinematic viscosity
σ	dimensionless complex decrement, $\sigma_r + i\,\sigma_i$
$\bar{\sigma}$	Stefan–Boltzmann constant
τ_o	optical thickness, $k_m D$.

Superscripts

$\bar{}$	base flow quantity
$\tilde{}$	perturbed quantity
$'$	dimensional quantity.

Subscript

i	cold wall, $i = 1$ at $x = 0$; hot wall, $i = 2$ at $x = 1$.

The first theoretical study of the stability of the conduction regime was carried out by Arpaci and Bayazitoglu [16]. An approximate formulation of the equation of radiative transfer which permits a formulation involving only a differential equation (P1 approximation) was used because of its simplicity. Thus, in addition to the Grashof number, the stability characteristics of a radiating gas layer depend on four parameters: the optical thickness τ_o, the interaction parameter or Planck number P_0, the non-greyness η and the emissivities of the vertical plates. An important outcome of this study is that the critical Grashof number reaches a maximum when the optical thickness increases. For thick gases, radiation does not affect the onset of instability and the maximum is more pronounced for cases corresponding to non-grey gases and non-black boundaries. The decreases of P_0 or of the emissivities of the plates flatten the base temperature which, in turn, leads to a decrease of the vertical velocities. Consequently the onset of instabilities is delayed in the conduction regime since the instabilities are produced by the shearing forces between the upward and downward flowing streams. This effect has also been shown in two-dimensional numerical calculations [14].

The stability of the conduction regime of radiating gases contained inside slender slots and subjected to either prescribed wall temperatures or convective boundary conditions has been studied by Hassab and Özisik [17]. An identical formulation of the radiating part of the problem was employed and the previous results were reinforced for the vertical case. In recent papers [18–20], the initial state was investigated in the convection regime and the base flow solution was found to agree with the numerical results obtained around the midheight of high aspect ratio cavities with a two-dimensional computational code. Also, it has been shown that the principle of exchange of stabilities does not hold in the conduction regime for asymmetric radiative boundary conditions or if the radiation term in the base flow equations is not linearized. For these cases, the instabilities set in as a single travelling wave the moving direction of which is strongly dependent on the emissivities of the bounding walls.

To date, the stability of the convection regime in radiating gases has not been treated in detail. The purpose of this study is to examine the effects of radiation on the stability properties of the transition and boundary layer regimes. Most of the results are restricted to cases for which radiative transfer and natural convection are of the same order of magnitude. In the following sections we present the basic system to be solved first. An extension is made to the application of the P3 approximation method for the radiation part of the problem in order to consider the improvement to be brought to the previous P1 results, especially at intermediate optical thicknesses. The dependence of the critical quantities upon the stratification parameter and the four radiation parameters quoted above is discussed next.

BASE FLOW SOLUTION

Consider the parallel flow of an absorbing, emitting, non-grey viscous fluid within a vertical channel. The side walls located at $x' = 0$ and D are taken opaque, grey and diffuse and are held at uniform temperatures T'_c and T'_h, respectively, with $T'_h > T'_c$. A Cartesian coordinate system is chosen with the positive z'-axis in the direction opposite to the gravity vector $\mathbf{g}$. It is assumed that the temperature difference $\Delta T' = T'_h - T'_c$ is small enough such that the Boussinesq approximation is valid and that viscous dissipation is negligible. The governing equations are put into non-dimensional form by introducing the set of scales (D, $\nu/g\beta\Delta T' D$, $\Delta T'$, $n^2\bar{\sigma}T'^3_m\Delta T'$) for length, time, temperature and radiative flux (or first moment of the radiation intensity), respectively. Assuming that a stable vertical temperature gradient γ is found in the core, the equations governing the plane-parallel flow may be obtained from the general formulation by setting

$$\begin{aligned} p &= \bar{p}(z) \\ \mathbf{V} &= [0, \bar{w}(x)] \\ T(x,z) &= \bar{T}(x) + \gamma z \\ \mathbf{q}_r &= (\bar{q}_{rx}, 0). \end{aligned} \tag{1}$$

The dimensionless equations governing the initial motion then reduce to

$$\frac{d^3\bar{w}}{dx^3} + \frac{d\bar{T}}{dx} = 0 \tag{2}$$

$$4m^4\bar{w} - \frac{d^2\bar{T}}{dx^2} + \frac{\tau_o}{P_0}\frac{d\bar{q}_{rx}}{dx} = 0 \tag{3}$$

subject to boundary conditions

$$\bar{w} = 0, \quad \bar{T} = T_m \pm 0.5 \quad \text{at } x = 0, 1. \tag{4}$$

In equation (3) m is the stratification parameter defined by $4m^4 = Ra\gamma$. The positive sign in equation (4) and in the subsequent equations is for the surface at $x = 1$. In these equations, the pressure has been eliminated by deriving the equation of motion. Consequently, a supplementary condition must be used to insure the closure of the system. In order not to force the velocity to be zero at $x = 0.5$, the third condition applied to the equation of motion is deduced from a mass flux over any cross-section

$$\int_0^1 \bar{w}(x)\,dx = 0. \tag{5}$$

The first- and third-order spherical harmonics method [21] modified in order to include the weighted effect of nongreyness [16] have been used to calculate the radiative flux in the energy equation.

If the radiation part is solved by the P1 approximation, the radiative flux is given by

$$\frac{d^2\bar{q}_{rx}(x)}{dx^2} - 3\tau_o^2\bar{q}_{rx}(x) - \frac{4\tau_o\eta}{T_m^3}\frac{d\bar{T}^4(x)}{dx} = 0 \tag{6}$$

which is subject to boundary conditions

$$\bar{q}_{rx} \pm \frac{4\lambda_i}{\eta\tau_o}\frac{d\bar{q}_{rx}}{dx} = 0 \quad \text{at } x = 0, 1. \tag{7}$$

When using the P3 approximation, the following equation must be solved:

$$\frac{d^4\bar{q}_{rx}}{dx^4} - 10\tau_o^2\frac{d^2\bar{q}_{rx}}{dx^2} + \frac{35}{3}\tau_o^4\bar{q}_{rx} - 4\tau_o\frac{\eta}{T_m^3}\frac{d^3\bar{T}^4}{dx^3} + \frac{140}{g}\tau_o^3\frac{\eta}{T_m^3}\frac{d\bar{T}^4}{dx} = 0. \tag{8}$$

At wall i, the boundary condition may be stated as

$$\begin{aligned} &-\frac{d^3\bar{q}_{rx}}{dx^3} + \frac{37}{3}\tau_o^2\frac{d\bar{q}_{rx}}{dx} \pm \frac{56}{9\lambda_i}\tau_o^3\eta\bar{q}_{rx} + 4\tau_o\frac{\eta}{T_m^3}\frac{d^2\bar{T}^4}{dx^2} = 0 \\ &15(1+\varepsilon_i)\gamma_i\frac{d^3\bar{q}_{rx}}{dx^3} \pm 32\gamma_i\tau_o\eta\frac{d^2\bar{q}_{rx}}{dx^2} \\ &\quad + \frac{5}{3}\tau_o^2[7 - 90(1+\varepsilon_i)\gamma_i]\frac{d\bar{q}_{rx}}{dx} \pm \frac{80}{3}\gamma_i(7\varepsilon_i - 19) \\ &\quad \times\tau_o^3\eta\bar{q}_{rx} - 60(1+\varepsilon_i)\gamma_i\tau_o\frac{\eta}{T_m^3}\frac{d^2\bar{T}^4}{dx^2} \\ &\quad \mp\left[-128\gamma_i\tau_o^2\frac{\eta^2}{T_m^3}\frac{d\bar{T}^4}{dx}\right] = 0 \end{aligned} \tag{9}$$

where

$$\gamma_i = 1/(5 - 3\varepsilon_i) \quad \text{and} \quad \lambda_i = \varepsilon_i/2(2 - \varepsilon_i), \quad i = 1, 2.$$

For the non-radiating case, the exact solution for the basic state can be readily found. Also, analytical solutions have been determined in the conduction regime for radiating fluids but by linearizing the non-linear term contained in equation (6) [16, 17]. On the other hand, the algebraic involvement with the solution of the base flows corresponding to the convection regimes should be a formidable task especially when using the P3 approximation. Moreover, the radiation term should be linearized and we shall show afterwards that this procedure has a clear influence on the stability calculations. Consequently, it is preferable to solve the basic equations numerically. At this point, it is appropriate to anticipate somewhat the contents of the next section: following the classical approach for stability problems, the disturbance variables will be expanded into a finite series of complete orthogonal trial functions to obtain approximate solutions of the eigenvalue problem. Since the solution of the basic state has to be introduced in the perturbation equations, it is desirable that the approximate solution of the initial problem should be expressed in terms of identical trial functions in order to simplify the treatment of the perturbation equations. In this study, Chebyshev polynomials were chosen to improve convergence [22]. Accordingly, the solution is expanded as

$$\bar{f}(x) = \sum_{n=0}^{N} f_n T_n^*(x) \tag{10}$$

where T_n^* is the nth-degree shifted Chebyshev polynomial of the first kind and $\tilde{f}$ stands for $\tilde{w}$, $\tilde{T}$, $\tilde{q}_{rx}$. Truncating each of the series to N terms and requiring the residuals to be orthogonal to each expansion function with the usual weight leads to a non-linear system for the expansion coefficients [18].

The general systems of equations were solved using the DGEFS routine from the SLATEC Library and the computations were performed in double precision on a VAX 11/780 computer. Concerning the number of terms which must be retained in the polynomial expansions, it has been found that N depends both upon the strength of the non-linear coupling between the energy and radiative transfer equations and upon the value of the stratification parameter. For example, in the boundary layer regime and for $\tau_o = 1$ the numerical method generates fourth decimal place accuracy when truncating the series to 12 terms only while an apparent limiting value is achieved with $N = 18$. For larger optical thicknesses, the radiative flux varies steeply at the walls. Consequently, more terms are required to obtain a given accuracy. For most of the computations presented herein, the number of terms ranges from 18 to 24.

The influence of radiation on the temperature profile is only mentioned here because it could be derived from previous literature: smaller temperature gradients are found in the middle of the layer and larger gradients near the boundaries. Decreases of the Planck number produce increases of these effects for all optical thicknesses with a maximum for $\tau_o \simeq 1$. Radiation becomes unimportant for small optical thicknesses ($\tau_o \simeq 0.1$ if $P_0 > 0.1$) and the problem may be assumed to be the one of a non-radiating fluid with a modified Prandtl number for large optical thicknesses since the radiative transfer tends towards a diffusive process. More interesting are the influences of radiation on the velocity field since the maximum velocities decrease or increase when increasing the relative importance of radiative heat transfer according to the value of the stratification parameter. For example, at $\tau_o = 1$, decreases of P_0 yield decreases in velocities if $m < 4.5$ while the opposite is seen in the boundary layer regime. It should also be noted that the velocity and temperature profiles are asymmetric with maximum velocities located within the cold side for black boundaries. This effect is due to the non-linear term in the energy equation. The influences of increases of the optical thickness are similar but with a maximum around moderate τ_o.

The accuracy of the P1 approximation has been studied by comparison with the P3 approximation. It is well established that the first-order approximation is not adequate for solving the two-dimensional equation of radiative transfer in square enclosures unless the medium is optically thick [21]. On the other hand the P3 approximation provides adequate results for $\tau_o > 0.5$. However, it should be noted that the large discrepancies obtained under radiative equilibrium conditions ($P_0 = 0$) and for cavities with moderate aspect ratios cannot challenge the validity of the results for the limiting one-dimensional coupled problem which corresponds with the basic flow. On account of the quite different points of view which can be found in the literature about this question, it was found appropriate to present selected comparisons between P1 and P3 results. Figure 1 shows velocity profiles for a moderate Planck number and $\tau_o = 1$ in the three flow regimes: the largest deviations are obtained in the conduction regime since P_0 is only a dimensionless measure of the relative importance of radiative and conductive heat fluxes and they are kept within a few percent. The discrepancies are much less expressed for the temperature while they are more important for the radiative heat flux. This can be seen in Fig. 2 especially around optical thicknesses of one. For the most unfavorable case considered in this study, the discrepancies in the velocities are about 10% while the radiative transfer produces a decrease of the maximum velocities of about 40%. In conclusion, it is believed that the P1 approximation is accurate enough to provide all the general trends on the effects of radiation for participating media enclosed in tall cavities. The increased complexity in the high-order approximations and the required computational efforts are only justified in radiation-dominated cases. The relevance of the stability computations could then be questionable.

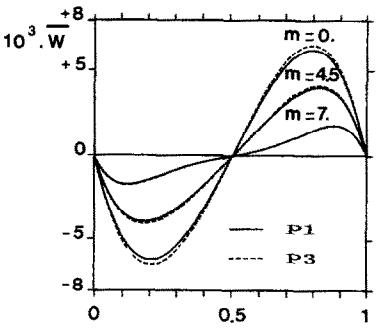

FIG. 1. Comparison of velocity profiles for the P1 and P3 approximations ($P_0 = 0.5$, $\tau_o = 1$, $\varepsilon_1 = \varepsilon_2 = 1$, $\eta = 1$, $Pr = 0.7$).

LINEAR STABILITY ANALYSIS

To investigate the stability of the basic flow, we follow the conventional approach in linear theory of superimposing arbitrarily small perturbations on the base flow velocities, pressure, temperature and radiative flux or first moment of the radiation intensity $\bar{I}_0$ according to

$$\tilde{q}_{rx} = -\frac{\eta}{3\tau_o}\frac{d\bar{I}_0}{dx}. \tag{11}$$

Thus the four variables are considered to be the sum of base flow (denoted by bars) and disturbance quantities (denoted by tildes) as follows:

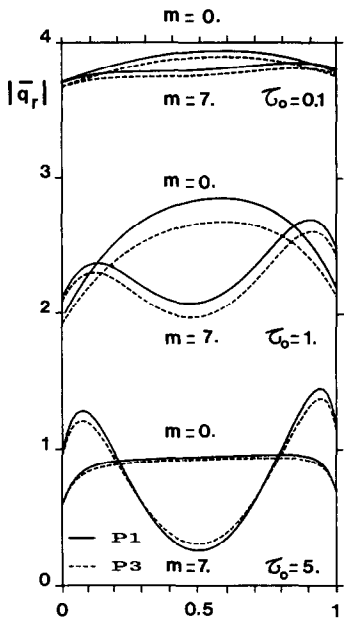

FIG. 2. Comparison of radiative heat flux distributions for the P1 and P3 approximations ($P_0 = 1$, $\varepsilon_1 = \varepsilon_2 = 1$, $\eta = 1$, $Pr = 0.7$).

$$(v, w, p, T, I_0) = (0, \tilde{w}, \tilde{p}, \tilde{T}, \tilde{I}_0) + \varepsilon(\tilde{v}, \tilde{w}, \tilde{p}, \tilde{T}, \tilde{I}_0), \quad \varepsilon \ll 1. \quad (12)$$

The perturbation equations are obtained by introducing the total quantities into the system of equations of the initial state cast in the stream function–vorticity formulation (ψ, Ω), then subtracting the base flow equations from the resulting equations and finally neglecting the perturbation terms of second and higher orders.

It should be stressed that the perturbed flow is obtained by considering that the parallel base flow can only be perturbed through two-dimensional infinitesimal disturbances in the x–z plane. The dependence of the perturbation quantities on x, z, t is written as a superposition of Fourier modes of the form

$$\tilde{f}(x, z, t) = f(x) \exp(\mathrm{i}\alpha z + \sigma t). \quad (13a)$$

A temporal analysis being undertaken, the decrement $\sigma = \sigma_r + \mathrm{i}\sigma_i$ is complex while the wave number α in the vertical direction is real. The wave speed c and the wavelength λ_d of the disturbances are given by

$$c = -\sigma_i/\alpha \quad (13b)$$

$$\lambda_d = 2\pi/\alpha. \quad (13c)$$

If $c = 0$, the disturbance mode is stationary and it is a travelling wave otherwise. The amplification rate of the Fourier mode is denoted by σ_r. The perturbation equations can be written as

$$0 = (\mathscr{D}^2 - \alpha^2)\psi - \Omega \quad (14)$$

$$\sigma Gr\,\Omega = \{(\mathscr{D}^2 - \alpha^2) - \mathrm{i}\alpha Gr\,\tilde{w}\}\Omega + \mathscr{D}T + \mathrm{i}\alpha Gr\,\mathscr{D}^2\tilde{w}\psi \quad (15)$$

$$\sigma Ra\,T = \{(\mathscr{D}^2 - \alpha^2) - \mathrm{i}\alpha Ra\,\tilde{w}\}T - 4m^4\mathscr{D}\psi + \mathrm{i}\alpha Ra\,\mathscr{D}\tilde{T}\psi + \frac{\eta}{3P_0}(\mathscr{D}^2 - \alpha^2)I_0 \quad (16)$$

$$0 = \{(\mathscr{D}^2 - \alpha^2) - 3\tau_o^2\}I_0 + 48\tau_o^2 \frac{\tilde{T}^3}{T_m^3}T \quad (17)$$

where

$$\mathscr{D} = \mathrm{d}/\mathrm{d}x.$$

The boundary conditions at $x = 0, 1$ are

$$\psi = \mathscr{D}\psi = 0, \quad T = 0, \quad \mathscr{D}I_0 \pm \frac{3\lambda_i\tau_o}{\eta}I_0 = 0. \quad (18)$$

This set of equations is solved by the spectral tau method with shifted Chebyshev polynomials of the first kind as trial functions. The four variables Ω, ψ, T, I_0 are expanded according to equation (10). Substituting the expansions into equations (14)–(17) and requiring the residuals to be orthogonal to the trial functions leads to a complex algebraic eigenvalue problem [19] which must be completed with equations (18) since the trial functions do not satisfy the boundary conditions.

This system can be written in matrix form as

$$A\mathbf{X} = \sigma B\mathbf{X}. \quad (19)$$

The vector $\mathbf{X}$ consists of the coefficients of the series. Matrix A is complex and B real.

The parameters which control the stability problem in the system of equations (14)–(17) are the Grashof number, the Prandtl number, the stratification parameter, the four radiation parameters P_0, τ_o, η, ε_i and the wave number. The condition for solving the above system generates an eigenvalue relation of the form $Gr(Pr, m, P_0, \tau_o, \eta, \varepsilon_i, \alpha) = 0$. The eigenvalue σ is a measure of the decay or amplification of the disturbances: depending on whether σ_r is positive, zero or negative, the disturbance is amplified, neutral or damped out; the curves of marginal stability are reached for $\sigma_r = 0$. Each point on these curves was constructed by applying a secant method of iteration to Gr with α fixed by satisfying the requirement that the real part of the highest eigenvalue equal to zero within a specified error for the Grashof number (errors less than 0.5%). According to the value of σ_i at this point, the flow is subject to stationary instability ($\sigma_i = 0$, exchange of stabilities) or to travelling wave instability ($\sigma_i \neq 0$, overstability). The critical Grashof numbers, Gr_c, and the critical wave numbers, α_c, correspond to the absolute minimum of the neutral curves. These minima were determined using a spline interpolation method.

DISTURBANCE ENERGY BALANCE

The power integral method, based on a balance of energy which takes into account the base flow distorsion due to the Reynolds stress and the buoyancy forces, gives additional insight into the physical process involved in the onset of instability. Indeed, at the critical points, the rate of transfer of kinetic energy from the total flow into the disturbances precisely balances the rate at which the energy of the disturbances is lost due to the viscous dissipation.

Following ref. [5], we obtain by applying the power integral method on the momentum equation

$$\sigma_r Gr E_k^* = Gr \Sigma_1^* + \Sigma_2^* - \Sigma_3^* \quad (20)$$

where the expression for $E_k^*, \Sigma_2^*, \Sigma_3^*$ are given in the Appendix. In equation (20), the term on the left-hand side represents the rate of growth of the disturbance kinetic energy. The energy source terms are $Gr\Sigma_1^*$, the rate of transfer of kinetic energy from the total flow to the disturbance due to Reynolds stress (shear forces), and Σ_2^*, the rate of transfer of kinetic energy to the disturbance due to the buoyancy forces. The term $-\Sigma_3^*$ is always negative (sink term) and gives the rate of loss of kinetic energy of the disturbance due to viscous dissipation. On the neutral curves an equilibrium flow is possible and we have

$$\Sigma_3^* = Gr \Sigma_1^* + \Sigma_2^*. \quad (21)$$

By studying the sign and the relative magnitudes of $Gr\Sigma_1^*$ and Σ_2^*, the main contribution to the disturbance kinetic energy can be found. In the following subsections, equation (21) will be normalized by dividing the two sides by Σ_3^*. Therefore, by setting $\Sigma_1 = \Sigma_1^*/\Sigma_3^*$ and $\Sigma_2 = \Sigma_2^*/\Sigma_3^*$, the sum $Gr\Sigma_1 + \Sigma_2$ must be equal to unity (within a prescribed numerical error) at the neutral points.

RESULTS

The numerical results were obtained for radiative parameters considered reasonable for gases and for a maximum temperature difference between the vertical side walls equal to 20% of the reference temperature ($T_m = 5$) so that the Boussinesq approximation might be valid. The Prandtl number was taken to be 0.7 for all the cases presented here. This value is representative of radiating gases such as carbon dioxide or ammonia at atmospheric pressure in the temperature range 300–500 K but slightly low for water vapour ($Pr \simeq 1$). For the Planck number, the smallest value was $P_0 = 0.1$. This is somewhat greater than the values used in previous stability studies [16, 17] but still out of the range corresponding to usual gases [13]. The domains of variations chosen for τ_o and η also appear to be representative of gases.

Stability calculations

In order to reduce the number of independent parameters, we will first consider grey media ($\eta = 1$) between black isothermal walls ($\varepsilon_1 = \varepsilon_2 = 1$). The neutral curves for values of stratification parameters relevant to the three flow regimes and for various Planck numbers at moderate optical thickness are shown in Fig. 3. The first significant effect of radiation is found in the nature of the disturbances. For a non-radiating fluid with $Pr = 0.7$, stationary wave disturbances govern the onset of instability if $m < 5$ while a transition to travelling wave instability occurs at the higher stratification corresponding to the boundary layer regime (the beginning of this regime being characterized by a negative horizontal temperature gradient at the centre-line of the channel). On the other hand, the odd-symmetry of the base flow being destroyed by radiation, the neutral Grashof number is always determined by travelling wave disturbances, even in the conduction regime. The second effect of radiation is to shift upward the neutral curves in the conduction regime. By decreasing P_0, the increase in critical Grashof number, Gr_c (denoted by dashes on the neutral stability curves), occurs continuously as can be seen in Fig. 3(a). It should be added that the critical Grashof numbers depend weakly upon the formulation used for the radiation term (linearized or not). Also, the critical wave speeds are much less than the maximum velocities of the base flow [20]. In the transition regime and at stratification parameters for which radiation increases the base flow velocities, the neutral stability curves are shifted downward (Fig. 3(b)). In these cases, the energy for instability is derived mainly from the shear forces at the midplane between the upstream and downstream flows. As shown in Fig. 3(b), radiation then plays a much more influential role on the stability characteristics of the flow: the variation of Gr_c with increasing radiation effects is more pronounced than its counterpart in the conduction regime. Conversely, at the higher temperature stratifications corresponding to the boundary layer regime, Fig. 3(c) shows that radiation stabilizes anew the flow against travelling wave disturbances. For $m = 10$, the curves have two minima for $P_0 > 1$. This type of transition was discussed in detail by Bergholz [5]. The high-wave number minimum is mainly associated with the shear forces (hydrodynamic instabilities) while the buoyancy forces prevail at the low-wave number minimum. To determine the dominant source of instabilities, energies of the disturbance have been calculated at the minima as a function of P_0 (Table 1). In a non-radiating fluid, the largest contribution to the disturbance kinetic energy comes from the buoyancy forces ($\Sigma_2 > Gr\Sigma_1$) at the critical points. By increasing the radiation effects, the shear mode instability becomes the more dangerous as can be seen from the increases of $Gr\Sigma_1$. Consequently, the main contributor to the disturbance kinetic energy is the shear force for a radiating gas having a moderate optical thickness at $m = 10$ and for $P_0 < 5$.

The variations of Gr_c with m and P_0 is shown in Fig. 4. The dashed curve represents the stationary

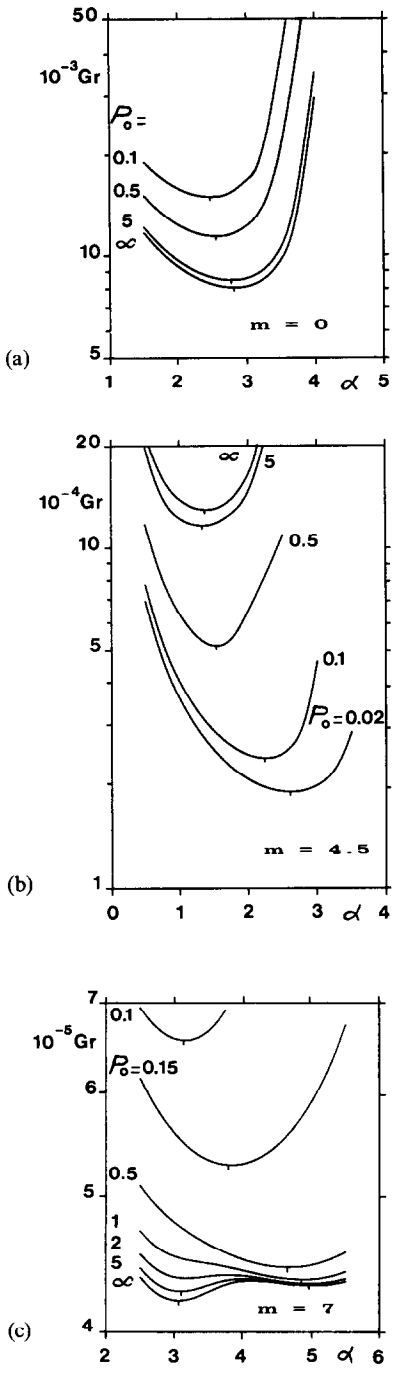

FIG. 3. Neutral stability curves for various P_0. Dashes denote the minimum ($\tau_o = 1, \eta = 1, \varepsilon_1 = \varepsilon_2 = 1, Pr = 0.7$): (a) conduction regime; (b) transition regime; (c) boundary layer regime.

mode for a non-radiating gas (conduction and transition regimes). The above discussed effects of radiation according to the flow regime are clearly illustrated on this figure. Due to the increasing difficulties involved in working out accurately the critical quantities, the calculations were restricted to Gr_c below about 10^6 for the m-values corresponding to the change from the transition to the boundary layer regime. Nevertheless, from the decrease of the slope of the left-hand branch of the stability curve which occurs when decreasing P_0, it can also be deduced that the domain of multicellular flows in the transition regime is spread out towards higher stratification parameters. It may be added that the horizontal temperature gradient in the midplane has a positive value as long as the critical point lies on this branch.

The variations of the critical wave number with m and P_0 are displayed in Fig. 5. A decrease in P_0 leads to a decrease in α_c for the low stratifications at which the critical quantities depend weakly on m. The behaviour of the wave number is then similar to that of a non-radiating fluid although the decrease with m becomes slower when decreasing P_0. As m increases above a particular value depending on P_0, the wave number rises sharply at first and then increases continuously with m if $P_0 < 0.5$. The drop in α_c due to the predominance of the buoyancy forces (at $m = 9.25$ in the non-radiating case) is obtained at higher m-values when P_0 decreases and disappears at $P_0 = 0.5$ in the range of temperature stratifications investigated. Figure 6 shows the variations of the maximum base flow velocity, $\bar{w}_{max}$, and critical wave speed, c, with m. It should be noted that the instabilities set in as a single travelling wave moving downwards for the radiating cases. As can be seen, the wave speeds are much less than the maximum of the base flow velocities and quite independent of m over most of the transition regime. In the range of m which corresponds to the end of this regime, the critical data were not computed as explained above ($Gr_c > 10^6$). A speed jump should be obtained followed by a decrease similar to that of $\bar{w}_{max}$. The wave speed is then higher than the speed of the two oppositely travelling waves relating to the non-radiating case until the point at which the low-wave number minimum determines the critical quantities ($m = 9.25$). The reverse is seen after this point. A sampling of the values of the critical parameters and relative magnitudes of the energy terms for the case $P_0 = 0.1$ are listed in Table 2. It is shown that the disturbances derive almost all their energy from the work of the shear forces, at least over the range of temperature stratifications investigated. Small positive contributions to the buoyancy forces are obtained when m is small like in the radiation-free problem. At larger values of m, the buoyancy term again becomes positive but Σ_2 is smaller than the shear stress production term.

The variation of the critical Grashof number with respect to the optical thickness is displayed in Fig. 7 for values of the stratification parameter corresponding to the three flow regimes and for $P_0 = 0.5$ and 0.1. In the conduction regime, Gr_c is observed at first to increase and then to decrease with τ_0. The critical Grashof number of the radiation-free problem is nearly reached at $\tau_o = 7$ and the maximum is obtained around an optical thickness of one. The critical wave number also assumes a minimum for $\tau_o \simeq 1$ while the critical wave speed is maximum. Similar

Table 1. Influence of the interaction parameter on the disturbance energy ($m = 10.0$, $\eta = 1.00$, $\tau_o = 1.00$, $\varepsilon_1 = \varepsilon_2 = 1.0$)

	Low wave number				High wave number			
P_0	α_c	Gr_c	$Gr\Sigma_1$	Σ_2	α_c	Gr_c	$Gr\Sigma_1$	Σ_2
0.10	—	—	—	—	3.15	657651	0.955	0.042
0.15	—	—	—	—	3.83	532289	0.911	0.086
0.50	—	—	—	—	4.655	447032	0.844	0.156
1.00	—	—	—	—	4.84	437395	0.830	0.170
2.00	3.16	438361	0.556	0.443	4.95	434376	0.825	0.175
5.00	3.09	428761	0.515	0.485	5.01	433062	0.821	0.179
∞	3.06	422129	0.491	0.509	5.05	432492	0.819	0.182

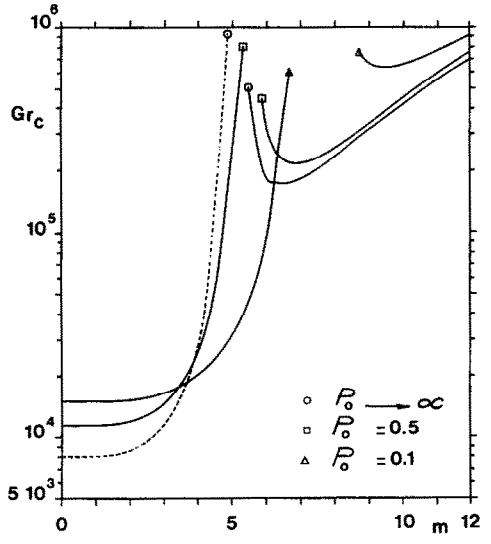

FIG. 4. Variation of the critical Grashof number with the stratification parameter: ----, stationary modes; ——, travelling modes ($\varepsilon_1 = \varepsilon_2 = 1$, $\eta = 1$, $\tau_o = 1$, $Pr = 0.7$).

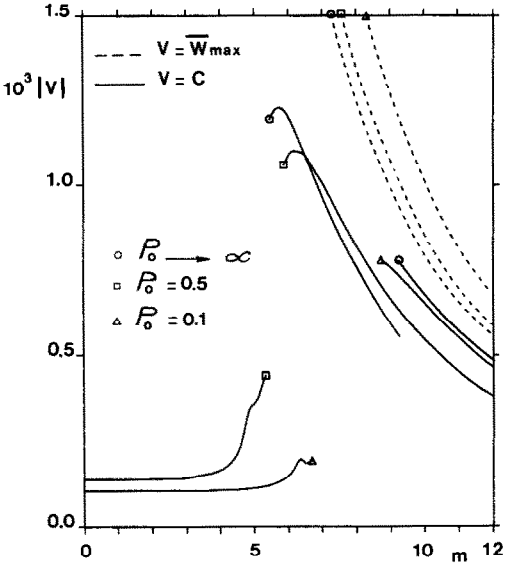

FIG. 6. Variation of the critical wave speed, —— c, and maximum base flow velocity, ---- $\bar{w}_{max}$, with the stratification parameter ($\varepsilon_1 = \varepsilon_2 = 1$, $\eta = 1$, $\tau_o = 1$, $Pr = 0.7$).

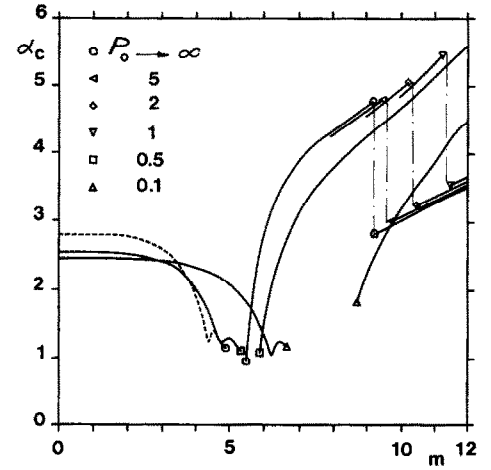

FIG. 5. Variation of the critical wave number with the stratification parameter: ----, stationary modes; —— travelling modes ($\varepsilon_1 = \varepsilon_2 = 1$, $\eta = 1$, $\tau_o = 1$, $Pr = 0.7$).

variations of Gr_c were reported previously [16, 17]. The additional feature to mention here is that the radiating case cannot be reduced to the non-radiating case for an optically thick gas when the radiation part is not linearized because the speed of the single wave, travelling in the direction of gravity, tends toward a constant value. In the transition regime, $m = 4.5$, radiation strongly destabilizes the flow at intermediate optical thicknesses and the drop in Gr_c becomes more pronounced when decreasing P_0. For $\tau_o > 2$, dependencies of Gr_c upon τ_0 and m are weaker. The increases of Gr_c which are shown at low values of τ_o can be explained by the particular m-value chosen. Indeed for $m = 4.5$, the base flow velocities are reduced for optically thin gases. Thus the onset of shear driven instabilities is delayed. At $m = 7$, rapid increases of Gr_c are obtained for moderate optical thicknesses. This stabilizing effect of radiation is due to the change-over in the mode of instability: the contribution of the work buoyancy forces to the disturbance kinetic energy decreases as τ_o increases. In contrast, the horizontal temperature gradient of the basic state in the midplane being positive for larger values of τ_o, the flow re-enters the transition regime at $\tau_o \simeq 1$ for $P_0 = 0.1$ and $\tau_o \simeq 2$ for $P_0 = 0.5$. A reversal of the effect of radiation is obtained then as can be seen from the slope of the right-hand branches of the Gr_c curves at $m = 7$. In summary, the results presented in Fig. 7 for various stratification parameters have shown that

Table 2. Critical values and disturbance energy for non-radiating fluid and for coupled radiation–convection ($Pr = 0.7$)

m	α_c	Gr_c	$10^3 c$	$Gr\Sigma_1$	Σ_2
		(a) $P_0 \to \infty$			
0.00	2.81	8030	0	0.906	0.094
3.00	2.60	11476	0	0.960	0.040
4.50	1.37	129325	0	1.091	−0.091
4.80	1.19	518722	0	1.063	−0.063
5.50	0.94	506458	±1.194	1.039	−0.038
6.00	2.76	184659	±1.206	0.963	0.032
8.75	4.57	289915	±0.645	0.820	0.180
9.00	4.66	314460	±0.613	0.819	0.181
9.25	2.90	340099	±0.762	0.512	0.488
10.00	3.00	414903	±0.678	0.467	0.521
12.00	3.50	701384	±0.484	0.451	0.540
		(b) $P_0 = 0.1, \tau_o = 1, \eta = 1, \varepsilon_1 = \varepsilon_2 = 1$			
0.00	2.46	14934	−0.103	0.954	0.046
3.00	2.42	16423	−0.103	0.972	0.033
4.50	2.23	24126	−0.106	1.031	−0.030
6.00	1.35	90212	−0.147	1.140	−0.143
6.70	1.16	606140	−0.192	1.099	−0.099
8.75	1.81	755734	−0.781	1.023	−0.027
9.00	2.18	676679	−0.761	1.007	−0.013
10.00	3.15	657651	−0.656	0.954	0.042
12.00	4.47	920909	−0.468	0.877	0.119

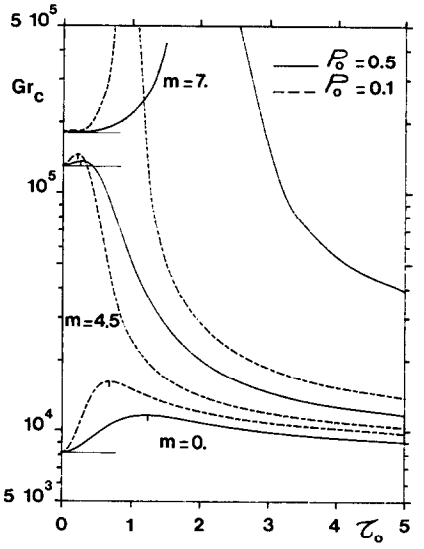

FIG. 7. Variation of the critical Grashof number with the optical thickness ($\varepsilon_1 = \varepsilon_2 = 1, \eta = 1, Pr = 0.7$).

stability of the flow is significantly improved at first by increasing the optical thickness while the opposite is true for values of τ_o exceeding a transition value which depends upon m as well as P_0. In the range of values of m and P_0 investigated, the transition was found to occur when $\tau_o \simeq 2$.

The critical Grashof numbers for m-values related to the three flow regimes ($m = 0, 4.5$ and 10) are listed in Table 3 for various non-greyness factors. Table 3(a) is for a moderate interaction ($P_0 = 0.5$) while Table 3(b) is for $P_0 = 0.1$. In the conduction regime, the results show that the onset of instability is delayed when η increases. In the transition regime, Gr_c decreases weakly at low η while increases are seen for $\eta > 0.8$. Since most of the disturbance energy is derived from the shear forces, this behaviour can be explained by decreases of the maximum base flow velocities which occur when η increases. At $m = 10$ (boundary layer regime both for $P_0 = 0.5$ and 0.1) the stability is more significantly improved for $P_0 = 0.1$. It can be noted that this effect depends upon the m-value chosen. Indeed, referring back to Fig. 4 ($\eta = 1$), it is seen that the critical curves show a minimum which moves towards both higher m and Gr_c values when P_0 decreases ($m = 6.9$, $Gr_c = 215914$ for $P_0 = 0.5$ and $m = 9.5$, $Gr_c = 638629$ for $P_0 = 0.1$). Gr_c declines sharply as long as this minimum is not reached while the slope of the critical curve is considerably less for m higher than the minimum value. At $P_0 = 0.5$ and $\eta = 1$, the critical point being located far above the minimum, variations of η in the range [0.5, 2] influence weakly the onset of travelling wave instability. On the other hand, the critical point for $m = 10$ is found to be close to the minimum of the critical curve for $P_0 = 0.1$ and $\eta = 1$. Therefore, Gr_c is highly sensitive to variations of the radiative parameters and Gr_c passes through the minimum with increasing η.

Finally, the influence of the wall emissivities ε_1 and ε_2 on the onset of instability are considered in this section. For low emissivities, it is well known from literature that the base flow temperature distribution becomes flatter with increasing relative importance of radiative transfer. This effect is expressed more in the case of one black wall and one reflecting wall owing to the availability of radiation reflected back to interact again with the fluid layer. As a result, the velocities are reduced, especially close to the wall the emissivity of which is the highest. These findings are valid whatever the flow regime considered. In order not to mix the effects of the non-linear term in the energy equation and those of the wall emissivities, the radiation part of the problem was linearized. In this case, the stability is improved by decreasing the wall emissivities. However, because of the dissymmetry of the base flow associated with different emissivities, travelling wave disturbances govern the onset of instability: a single travelling wave is obtained along the wall where the maximum base flow velocity occurs. In addition, since the non-linear formulation of the radiative term systematically leads to a negative wave speed, the critical wave speed is increased for a cold wall emissivity ε_1 lower than the hot wall emissivity, ε_2. On the other hand, the positive critical wave speed along the hot wall decreases when $\varepsilon_2 < \varepsilon_1$.

The effects of variations of wall emissivities upon the critical Grashof number and wave speed are displayed in Figs. 8 and 9. The critical quantities are given as a function of the stratification parameter for four cases. For identical emissivities, the critical

Table 3. Influence of the non-greyness factor on the critical values for selected stratification parameters

(a) $P_0 = 0.5$				(b) $P_0 = 0.1$			
η	α_c	Gr_c	$10^3 c$	η	α_c	Gr_c	$10^3 c$
		$m = 0$				$m = 0$	
0.50	2.68	9323	−0.108	0.50	2.53	11 052	−0.141
0.75	2.61	10 322	−0.126	0.75	2.47	12 965	−0.122
1.00	2.55	11 410	−0.137	1.00	2.46	14 952	−0.103
1.25	2.49	12 531	−0.142	1.25	2.45	16 860	−0.086
1.50	2.43	13 689	−0.145	1.50	2.44	18 802	−0.074
1.75	2.38	14 862	−0.144	1.75	2.43	20 725	−0.063
2.00	2.34	16 044	−0.143	2.00	2.43	22 623	−0.055
		$m = 4.5$				$m = 4.5$	
0.50	1.47	53 968	−0.193	0.50	2.15	23 327	−0.153
0.75	1.52	51 485	−0.207	0.75	2.20	23 281	−0.128
1.00	1.55	51 718	−0.214	1.00	2.24	24 126	−0.106
1.25	1.53	52 510	−0.125	1.25	2.27	25 337	−0.089
1.50	1.53	53 949	−0.213	1.50	2.29	26 760	−0.075
1.75	1.52	55 542	−0.211	1.75	2.30	28 291	−0.065
2.00	1.51	57 510	−0.206	2.00	2.31	29 885	−0.057
		$m = 10$				$m = 10$	
0.50	4.83	433 963	−0.535	0.50	3.94	490 376	−0.650
0.75	4.74	439 745	−0.545	0.75	3.53	560 113	−0.661
1.00	4.65	447 032	−0.548	1.00	3.15	657 651	−0.656
1.25	4.58	454 550	−0.549	1.25	2.76	795 597	−0.643
1.50	4.52	463 024	−0.549	1.50	2.31	1 014 604	−0.625
1.75	4.46	471 971	−0.549				
2.00	4.40	481 345	−0.549				

Grashof number increases when decreasing simultaneously ε_1 and ε_2 in the conduction and transition regimes. The influence of the radiative boundary conditions is less pronounced at higher stratification parameters ($m > 7$) since the relative importance of radiative heat transfer decreases. In the case of different wall emissivities, the most noticeable outcome of the study is the behavourial difference in the critical curves shown at the end of the transition regime ($4 \leqslant m \leqslant 6$). Unlike the previous results for the effects of the other radiative parameters, it can be seen on Figs. 8 and 9 that the flow is not rapidly stabilized against disturbances as the temperature stratification is greater than $m = 4$. Furthermore, for a black cold wall and a mirror hot wall ($\varepsilon_1 = 1, \varepsilon_2 = 0$), the onset of instability is monotonically increased with increasing m. Therefore, Gr_c is hardly reduced at the end of the transition regime in the case of dissymmetric radiative boundary conditions. It must also be emphasized that Gr_c is entirely determined by travelling wave disturbances as can be seen in Fig. 9. The critical wave speeds are increased in the conduction regime and assume a maximum at $m \simeq 6$ instead of the speed jumps discussed previously. On the other hand, calculations of the energies of critical disturbances have shown that changes in the radiative boundary conditions act slightly upon $Gr\,\Sigma_1$ and Σ_2. The main contribution to the disturbance kinetic energy comes from the viscous forces in the range $4 \leqslant m \leqslant 6$.

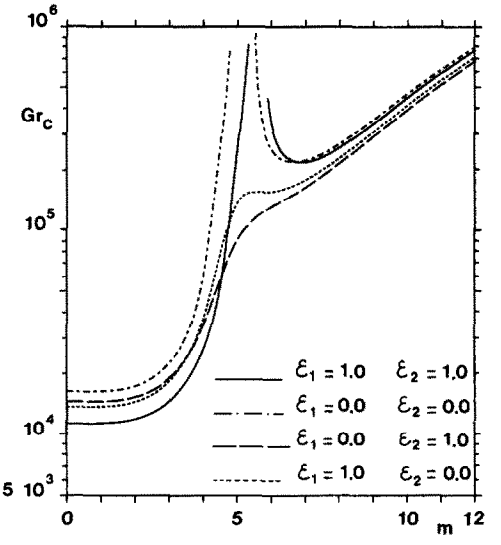

FIG. 8. Effects of wall emissivities on the critical Grashof number ($P_0 = 0.5$, $\tau_o = 1$, $\eta = 1$, $Pr = 0.7$).

NUMERICAL SIMULATIONS

Numerical simulations of flows in tall vertical cavities were performed in order to assess the stability calculations. The results discussed in this section complete those presented previously [11, 14, 15].

Following a procedure similar to the ones described in refs. [7, 23], the variations of the critical Grashof number with the aspect ratio can be obtained by combining the vertical gradient at the cavity midplane derived from numerical simulations and the critical data (Fig. 4). The resulting critical curves in the (Gr_c–A) plane shown in Fig. 10 are much more convenient for practical purposes since the stratification parameter is *a priori* unknown. Due to the lack of numeri-

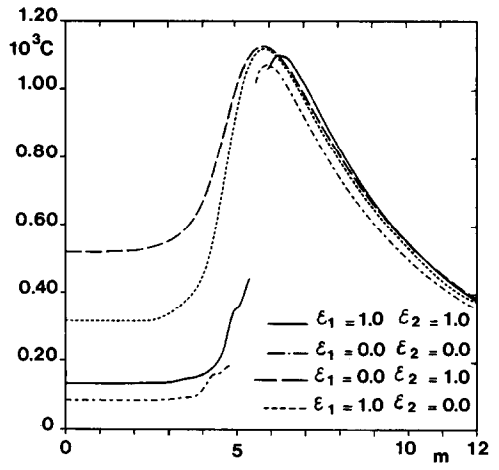

FIG. 9. Effects of wall emissivities on the critical wave speed ($P_0 = 0.5$, $\tau_o = 1$, $\eta = 1$, $Pr = 0.7$).

cal data for high Grashof numbers and high aspect ratio cavities in the radiating case, only one branch of the critical curves was plotted for $P_0 = 1$. As can be seen, the stabilizing effect supplied by the radiative transfer in the conduction regime is put in evidence. It should also be noted that the bottom part of the critical curve is nearly parallel to the A-axis. Therefore, unlike the non-radiating case, the critical Grashof number depends weakly on the aspect ratio for $A > 10$. In the transition regime, the increases in Gr_c are found in accordance with previous results of simulations [14, 15].

As pointed out before, the onset of instability is delayed in the transition regime when the aspect ratio of the cavity is lower than $A \simeq 12$ in the non-radiating case for fluid having $Pr = 0.7$. On the other hand, the critical aspect ratio for which multicellular flow is first expected in the transition regime is reduced to $A_c \simeq 10$ under the effect of radiation. Further decreases of

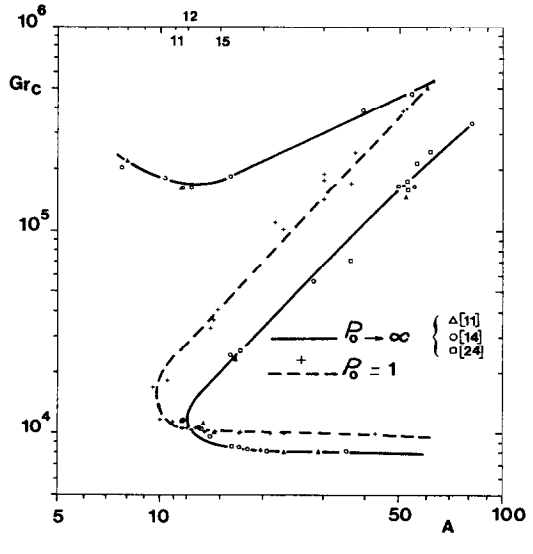

FIG. 10. Variation of the critical Grashof number vs aspect ratio ($\tau_o = 1$, $\eta = 1$, $\varepsilon_1 = \varepsilon_2 = 1$, $Pr = 0.7$).

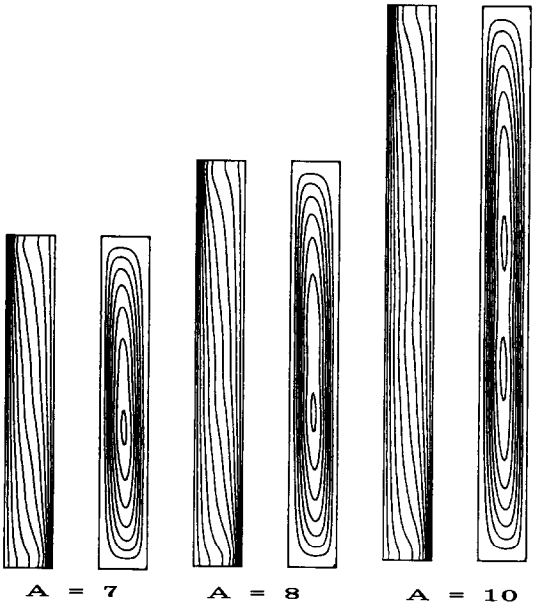

FIG. 11. Effects of aspect ratio on the isotherms and streamlines for a radiating fluid, $Gr = 15000$ ($P_0 = 0.5$, $\tau_o = 1$, $\eta = 1$, $\varepsilon_1 = \varepsilon_2 = 1$, $Pr = 0.7$).

P_0 will bring it down again as shown in Fig. 11 for $P_0 = 0.5$. At $Gr = 15000$, a weak multicellular flow is established at $A = 8$. The instabilities are strengthened when increasing A since the vertical temperature stratification in the region of the centre of the cavity becomes lower. This reduction of the critical aspect ratio can be explained by the general effect of the radiative transfer in participating media bounded by two isothermal walls: radiation makes the temperatures more uniform in the centre region while the temperature gradients are increased at the walls. Therefore, radiation compensates the stabilizing effects of the end regions as it was discussed by Lee and Korpela [10].

In the boundary layer regime, the theory predicts that the unicellular range should be stretched under the effects of radiation. An example may be used to shed light on the agreement between the numerical computations and stability analysis. From the streamlines reported in Fig. 12 for a cavity with $A = 10$ at $Gr = 200000$ it can be seen that cells have formed in the central region of a cavity filled with a non-radiating fluid. It should be noted that the secondary motions appearing in the end regions are steady and probably stem from the turning of the fluid in the ends. On the other hand, the monocellular flow persists at this Grashof number for $P_0 = 0.5$. The stratification at cavity midpoint is kept constant with $m = 6.36$. Similar numerical solutions were obtained by increasing the optical thickness at higher interaction parameters.

SUMMARY AND CONCLUSIONS

The stability of natural convection flows of radiating fluids contained inside vertical slots subjected

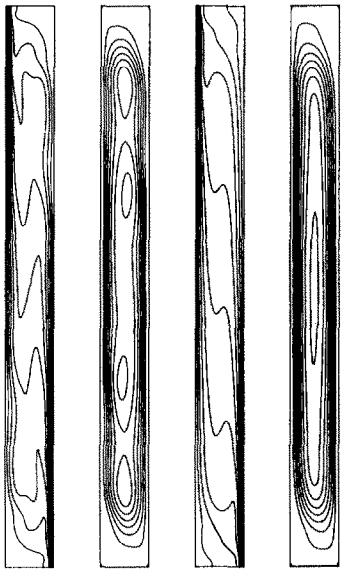

FIG. 12. Isotherms and streamlines in a cavity with $A = 10$ at $Gr = 200\,000$ ($\tau_o = 1$, $\eta = 1$, $\varepsilon_1 = \varepsilon_2 = 1$, $Pr = 0.7$).

to prescribed wall temperatures has been studied by means of linear stability analysis and by numerical methods. The critical parameters and the energies of the critical disturbances were determined for a wide range of radiative parameters. The critical instabilities were found to set in as a single travelling wave the moving direction of which is strongly dependent on the emissivities of the bounding walls. This is a consequence of the loss of the odd symmetry of the base flow. From the calculations of the energies of the disturbances it has been shown that the dominant source of instabilities in the transition and in the boundary layer regimes is due to the shear forces for a radiating gas having a moderate optical thickness. The following conclusions may be drawn from the stability analysis.

(1) Increasing the effect of radiation by decreasing the interaction parameter P_0 stabilizes the flow in the conduction regime. At the onset of instabilities, the wave speed is much lower than the maximum base flow velocities.

(2) On the other hand, radiation strongly destabilizes the flow in the transition regime.

(3) In the boundary layer regime, radiation produces a change over in the source of instability. The contribution of the work of the buoyancy forces to the disturbance kinetic energy decreases. Accordingly, a stabilizing effect of radiation is shown.

The stability of the flow is significantly improved at first by increasing the optical thickness while the opposite is seen for values of τ_o exceeding a transition value depending upon m as well as P_0. The influence of the non-greyness factor was found to be more complicated and no general trends can be drawn. The most noticeable outcome from the study of the influence of the wall emissivities is that the critical Grashof number is strongly reduced at the end of the transition regime in the case of dissymmetric radiative boundary conditions. The critical Grashof number monotonously increases then when increasing the temperature stratification.

To end, we have shown that the flow features that have been predicted by stability theory can be obtained by numerical simulations. In addition, by combining the results derived from stability calculations and numerical simulations, it has been shown that the critical aspect ratio at which a multicellular convection can take place in the transition regime is decreased by enhancing the radiative transfer.

The results presented here, although based on an approximate radiative transfer analysis, are expected to provide all the significant qualitative behaviours of the physical problem studied in this paper.

Acknowledgements—We are grateful to the CNAM for the support of this reaserch. The runs were performed in part at the CIRCE Computing Centre of the CNRS. Many thanks are due to the CIRCE for making their excellent computing facility available for the production runs.

REFERENCES

1. G. Z. Gershuni, Stability of plane convective motion of a liquid, *Zh. Tech. Fiz.* **23,** 1838–1844 (1953).
2. R. N. Rudakov, Spectrum of perturbations and stability of convection motion between vertical planes, *P.M.M.* **31,** 349–355 (1967).
3. R. V. Birikh, G. Z. Gershuni, E. M. Zhukhovitskii and R. N. Rudakov, On oscillatory instability of plane-parallel convective motion in a vertical channel, *P.M.M.* **26,** 745–748 (1972).
4. S. A. Korpela, D. Gözüm and C. B. Baxi, On the stability of the conduction regime of natural convection in a vertical slot, *Int. J. Heat Mass Transfer* **16,** 1683–1690 (1973).
5. R. F. Bergholz, Instability of steady natural convection in a vertical fluid layer, *J. Fluid Mech.* **84,** 743–748 (1978).
6. A. M. Shaaban and M. N. Özisik, The effect of nonlinear density stratification on the stability of a vertical water layer in the conduction regime, *J. Heat Transfer* **105,** 130–137 (1983).
7. J. E. Hart, Stability of the flow in a differentially heated inclined box, *J. Fluid Mech.* **47,** 547–576 (1971).
8. M. W. W. Schinkel, Natural convection in inclined air-filled enclosures, Ph.D. thesis, Delft University of Technology (1980).
9. I. P. Jones, A numerical study of natural convection in an air-filled cavity: comparison with experiment, *Numer. Heat Transfer* **2,** 193–214 (1979).
10. Y. Lee and S. A. Korpela, Multicellular natural convection in a vertical slot, *J. Fluid Mech.* **126,** 91–121 (1983).
11. G. Lauriat and G. Desrayaud, Natural convection in air-filled cavities of high aspect ratios: discrepancies between experimental and theoretical results, ASME 85-HT-37, Denver (1985).
12. J. C. Bratis and J. L. Novotny, Radiation–convection interaction in the boundary layer regime of an enclosure, *Int. J. Heat Mass Transfer* **17,** 23–36 (1974).
13. Y. Kurosaki, M. Mishina and T. Kashiwagi, Heat trans-

fer combined with radiation and natural convection in a rectangular enclosure. In *Proc. 7th Int. Heat Transfer Conf.*, Munich, Vol. 2, pp. 215–220 (1982).
14. G. Lauriat, Combined radiation–convection in gray fluids enclosed in vertical cavities, *J. Heat Transfer* **104,** 609–615 (1982).
15. G. Lauriat, Numerical study of the interaction of natural convection with radiation in nongrey gases in a narrow vertical cavity. In *Proc. 7th Int. Heat Transfer Conf.*, Munich, Vol. 2, pp. 153–158 (1982).
16. V. S. Arpaci and Y. Bayazitoglu, Thermal stability of radiating fluids : asymmetric slot problem, *Physics Fluids* **16,** 589–593 (1973).
17. M. A. Hassab and M. N. Ozisik, Effects of radiation and convective boundary conditions on the stability of fluid in an inclined slender slot, *Int. J. Heat Mass Transfer* **22,** 1095–1105 (1979).
18. G. Desrayaud and G. Lauriat, Natural convection of a radiating fluid in a vertical layer, *J. Heat Transfer* **107,** 710–712 (1985).
19. G. Desrayaud and G. Lauriat, On the stability of natural convection of a radiating fluid in a vertical slot, *Int. Commun. Heat Mass Transfer* **11,** 439–450 (1984).
20. G. Lauriat and G. Desrayaud, Influences of the boundary conditions and linearization on the stability of a radiating fluid in a vertical layer, *Int. J. Heat Mass Transfer* **28,** 1613–1617 (1985).
21. A. C. Ratzel and J. R. Howell, Two-dimensional radiation in absorbing–emitting media using the *P–N* approximation, *J. Heat Transfer* **105,** 333–340 (1983).
22. S. A. Orszag, Accurate solution of the Orr–Sommerfeld stability equation, *J. Fluid Mech.* **50,** 689–703 (1971).
23. B. Roux, J. C. Grondin, P. Bontoux and G. de Vahl Davis, Reverse transition from multicellular to monocellular motion in vertical fluid layer, PCH Madrid, pp. 1–6 (1980).
24. G. D. Raithby and H. H. Wong, Heat transfer by natural convection across vertical layers, *Numer. Heat Transfer* **4,** 447–457 (1981).

APPENDIX

Since we are only interested in the driving forces, the power integral method is applied on the momentum equation. Let ψ^* represent the complex conjugate of $\tilde{\psi}$, multiply the resulting equation from equations (14) and (15) by ψ^*, integrate over the interval [0, 1] and take only the real part of the derived expression.

Then we obtained, following Bergholz [5], equation (20)

$$\sigma_r Gr E_k^* = Gr\,\Sigma_1^* + \Sigma_2^* - \Sigma_3^*$$

where

$$E_k^* = -\frac{1}{2}\mathrm{Re}\left\{\int_0^1 \psi^*(\mathscr{D}^2-\alpha^2)\tilde{\psi}\,\mathrm{d}x\right\}$$

$$E_1^* = -\frac{\alpha}{2}\mathrm{Im}\left\{\int_0^1 \psi^*[(\bar{w}-c)(\mathscr{D}^2-\alpha^2)-\mathscr{D}^2\bar{w}]\tilde{\psi}\,\mathrm{d}x\right\}$$

$$E_2^* = -\frac{1}{2}\mathrm{Re}\left\{\int_0^1 \psi^*\mathscr{D}\hat{T}\,\mathrm{d}x\right\}$$

$$E_3^* = \frac{1}{2}\mathrm{Re}\left\{\int_0^1 \psi^*(\mathscr{D}^2-\alpha^2)^2\tilde{\psi}\,\mathrm{d}x\right\}$$

Re and Im being the real and the imaginary parts of the expressions.

INFLUENCE DU RAYONNEMENT SUR LA STABILITE DES ECOULEMENTS DANS DES CAVITES VERTICALES

Résumé—La stabilite des ecoulements de convection naturelle d'un fluide absorbant, émissif, non gris et non diffusant confine entre deux parois verticales chauffées différentiellement est étudié. L'équation de transfert radiatif est simplifiée en utilisant l'approximation P1. Les équations du mouvement de base et les équations de perturbation linéarisées sont résolues à l'aide de la méthode spectrale tau. L'effet du rayonnement sur les valeurs critiques est présenté en fonction du paramètre d'interaction, de l'épaisseur optique, du facteur spectral et des émissivités des parois pour une large gamme de valeurs du paramètre de stratification. L'énergie des modes critiques de perturbation est également calculée. Les instabilités se présentent toujours sous la forme d'une onde progressive dont la direction dépend de l'émissivité des parois. Les prédictions de l'analyse de stabilité linéaire sont confirmées par des simulations numériques.

DER STRAHLUNGSEINFLUSS AUF DIE STABILITÄT VON FLUIDEN IN VERTIKALEN HOHLRÄUMEN

Zusammenfassung—Es wird die Stabilität der natürlichen Konvektion eines strahlungsfähigen Fluids in einem vertikalen Spalt mit isothermen Seitenwänden unterschiedlicher Temperatur untersucht. Dabei wird ein absorbierend-emittierendes, nicht-graues, nicht-streuendes Fluid betrachtet und die P1-Näherung benutzt, um den Strahlungsfluß in der Energiegleichung zu beschreiben. Die grundlegenden Strömungsgleichungen und die linearen Stabilitätsgleichungen werden mit einer spektralen tau-Methode gelöst. Der Einfluß der Strahlung auf die kritischen Werte wird als Funktion des Wechselwirkungs-Parameters, der optischen Dicke des Fluids, des "Nicht-Grau"-Parameters und der Wand-Emission über einem weiten Bereich von Schichtungs-Parametern dargestellt. Die Energie-Inhalte der kritischen Stör-Arten werden ebenso berechnet. Für alle untersuchten Fälle ergab sich, daß die Instabilitäten als eine einzelne wandernde Welle einsetzen, deren Bewegungsrichtung von der Wand-Emission abhängt. Die Voraussagen der Stabilitätsanalyse von mehrzelligen Strömungen strahlungsfähiger Fluide werden mit Hilfe von Finite-Elemente-Berechnungen überprüft.

ВЛИЯНИЕ ИЗЛУЧЕНИЯ НА УСТОЙЧИВОСТЬ ЖИДКОСТЕЙ В ЗАМКНУТЫХ ВЕРТИКАЛЬНЫХ ПОЛОСТЯХ

Аннотация—Исследуется устойчивость естественной конвекции излучающей жидкости в вертикальной полости, изотермические боковые стенки которой имеют разные температуры. Рассматривается поглощающе–излучающая несерая и нерассеивающая среда. Лучистый поток в уравнении энергии учитывается с помощью P1 аппроксимации. Уравнения, описывающие течение, и уравнения линейной устойчивости решаются спектральным τ-методом. Влияние излучения на критические значения представлены в виде зависимостей от параметра взаимодействия, оптической толщины, параметра несерого состояния среды и степени черноты стенок в широком диапазоне значений параметра стратификации. Кроме того, рассчитан энергетический баланс критических мод возмущений. Для всех исследованных случаев найдено, что неустойчивость возникает в виде одиночной бегущей волны, направление движения которой зависит от степени черноты стенок. Результаты анализа устойчивости проверяются конечно-разностными расчетами многоячеистых течений излучающих жидкостей.